Low-Temperature Photoluminescence of Na^+(cryptand[2.2.2])Na^- Excited with a Picosecond Laser

Rodney S. Bannwart,[†,‡,§] Stuart A. Solin,[†,‡] Marc G. De Backer,[§,‡] and J. L. Dye*[,§,‡]

Contribution from the Department of Physics and Astronomy, Department of Chemistry, and Center for Fundamental Materials Research, Michigan State University, East Lansing, Michigan 48824. *Received January 13, 1989*

Abstract: Luminescence spectra of the crystalline alkalide Na^+(cryptand[2.2.2])Na^- were studied from 7 to 80 K. Dye laser excitation at wavelengths between 560 and 618 nm (2.2 and 2.0 eV) resulted in a narrow emission peak whose position varied from 669.1 nm (1.854 eV) at 7 K to 678.6 nm (1.828 eV) at 80 K. The intensity decreased markedly with increasing temperature, and the width (fwhm) increased from 30 to 60 meV. Time-resolved emission spectra at 7–9 K showed emission from at least two closely spaced levels. The initial emission peak is at 669 nm (1.86 eV) while at longer times (>10 ns) the peak shifts to 676.0 nm (1.835 eV). The results are compatible with excitation from a narrow $3s^2$ ground state band to a more diffuse 3s3p excited state and emission from the bottom of the p band to the ground state, accompanied by relaxation of the excited state to a slightly lower energy. There is also evidence for short-time emission from somewhat higher energy states.

It has been known for some time that alkali metals dissolve in ammonia to form solvated cations and solvated electrons, while alkali metals dissolved in aliphatic amines also contain solvated alkali metal-anions.[1] The use of cation complexing agents such as cryptands or crown ethers (see Figure 1) extended the range of solvents in which these solutions could be formed.[2,3] In 1974, it was shown that a new class of ionic solids could be precipitated from these solutions in which the positive species was a complexed cation and the negative species an alkali-metal anion.[4,5] These compounds, in which the anions are negative alkali-metal anions are called *alkalides* and have the general formula $M_a^+C_xM_b^-$, where M_a and M_b are alkali metals and C is a complexant. In some cases, by control of the stoichiometry and proper choice of solvent, M_b^- can be replaced by a trapped electron; these compounds form a class of compounds called *electrides*.[6] To date, over 30 alkalides and electrides have been synthesized and characterized.[7]

The optical spectra of thin films of alkalides are very similar to those of the corresponding alkali-metal anions in solution. Each consists principally of a band whose absorption peak depends on the nature of the anion. These peaks are centered at 650 nm for Na^-, 830 nm for K^-, 860 nm for Rb^-, and 950 nm for Cs^- as shown in Figure 2. Electrides are characterized by bands in the infrared[8,9] similar to those of solvated electrons in the case of "localized electrides" or to those of the plasmon absorption of concentrated metal–ammonia solutions for "delocalized" electrides.

Sodides (containing Na^-) are the most stable of these compounds. All alkalides and electrides are, however, unstable to irreversible decomposition so that the temperature of the samples used in the work reported here was always kept below −20 °C during synthesis and handling. Among the sodides, Na^+(C222)Na^- was the first to be crystallized and to have its structure determined by X-ray diffraction.[5] It is also reasonably stable and has been the most extensively studied.[10] [Na^+(C222)Na^- is stable for 1–2 days in vacuo at room temperature.] The unit cell of Na^+(C222)Na^- is rhombohedral and contains 3 formula units per unit cell in the hexagonal setting. The space group is $R32$ (no. 155, hexagonal setting), and the lattice parameters are $a = 4.415$ Å and $c = 14.63$ Å. The radius of the anion is about 2.7 Å, and the radius of the complexed cation is ~4.5 Å. The shortest anion–anion distances are 8.8 Å within the plane and 11.8 Å between Na^- ions in different planes.

Electronic studies of Na^+(C222)Na^- have revealed that it behaves as an intrinsic semiconductor with an apparent bandgap of 2.4 ± 0.1 eV[11] as determined by conductivity measurements in the temperature range 220–280 K. Magnetic, optical,[10] and EPR studies have shown that the concentration of trapped unpaired electrons for samples stored in the dark at temperatures below −40 °C is very small (barely detectable EPR signal, for example). This is unusual among the sodides, because most of the others are heavily doped with electrons (n type). This doping occurs during crystallization and cannot be prevented at the present time. Samples of Na^+(C222)Na^- show a dramatic increase in spin concentration upon illumination.[12]

Photoluminescence (PL) from single crystals of Na^+(C222)Na^- at room temperature irradiated with an attenuated argon ion laser beam at 488 nm (2.54 eV) was previously observed.[13] A single broad band (0.4 eV fwhm) with its maximum at 560 nm (2.2 eV) was obtained, and no emission corresponding to the region of the absorption maximum (650 nm, 1.91 eV) could be detected. Use of excitation wavelengths corresponding to the absorption maximum did not produce luminescence.[13]

In the present study, the photoluminescence spectrum was examined as a function of the temperature in the range 7–80 K, and the photoluminescence lifetime was studied as a function of emission wavelength at 7–9 K. This is the first report of low-temperature photoluminescence in any of the alkalides or electrides.

Experimental Section

Na^+(C222)Na^- was synthesized and purified as previouly described.[5] Weighed quantities of purified cryptand C222 and of sodium metal were loaded into a synthesis cell in a helium-filled glovebox. After evacuation of the cell to ~10^{-5} Torr, the metal was distilled from a side arm to form a shiny mirror on the cell wall. The complexation reaction was carried

[†] Department of Physics and Astronomy.
[‡] Center for Fundamental Materials Research.
[§] Department of Chemistry.

(1) For a review and additional references, see: Dye, J. L. *Prog. Inorg. Chem.* **1984**, *32*, 327–441.
(2) Dye, J. L.; DeBacker, M. G.; Nicely, V. A. *J. Am. Chem. Soc.* **1970**, *92*, 5226–5228.
(3) Dye, J. L.; Lok, M. T.; Tehan, F. J.; Coolen, R. B.; Papadakis, N.; Ceraso, J. M.; DeBacker, M. G. *Ber. Bunsen-Ges. Phys. Chem.* **1971**, *75*, 659–662.
(4) Dye, J. L.; Ceraso, J. M.; Lok, M. T.; Barnett, B. L.; Tehan, F. J. *J. Am. Chem. Soc.* **1974**, *96*, 608–609.
(5) Tehan, F. J.; Barnett, B. L.; Dye, J. L. *J. Am. Chem. Soc.* **1974**, *96*, 7203–7208.
(6) Huang, R. H.; Faber, M. K.; Moeggenborg, K. J.; Ward, D. L.; Dye, J. L. *Nature* **1988**, *331*, 599–601.
(7) Dye, J. L.; DeBacker, M. G. *Annu. Rev. Phys. Chem.* **1987**, *38*, 271–301.
(8) Dye, J. L.; Yemen, M. R.; Dague, M. G.; Lehn, J.-M. *J. Chem. Phys.* **1978**, *68*, 1665–1670.
(9) Dye, J. L.; Dague, M. G.; Landers, J. S.; Lewis, H. L. *J. Phys. Chem.* **1980**, *84*, 1096–1103.
(10) Jaenicke, S.; Faber, M. K.; Dye, J. L.; Pratt, Jr., W. P. *J. Solid State Chem.* **1987**, *68*, 239–246.
(11) Papaioannou, J.; Jaenicke, S.; Dye, J. L. *J. Solid State Chem.* **1987**, *67*, 122–130.
(12) DeBacker, M. G.; Dye, J. L., unpublished observations, this laboratory.
(13) Jaenicke, S.; Dye, J. L. *J. Solid State Chem.* **1984**, *54*, 320–329.

0002-7863/89/1511-5552$01.50/0

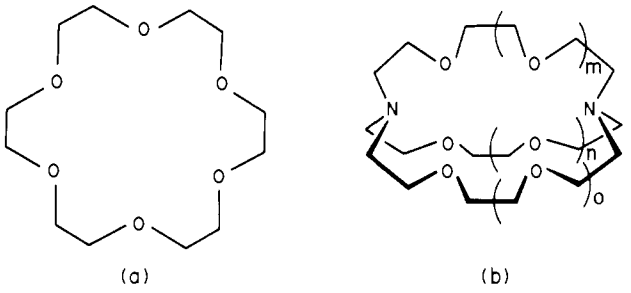

Figure 1. Representations of (a) 18-crown-6 and (b) cryptand[*p.q.r*] (*Cpqr*), with $p = m + 1$, $q = n + 1$, $r = o + 1$. The crown ethers form planar structures and the cryptands form three-dimensional cages. Cryptand[2.2.2] (C222) has $p = q = r = 1$.

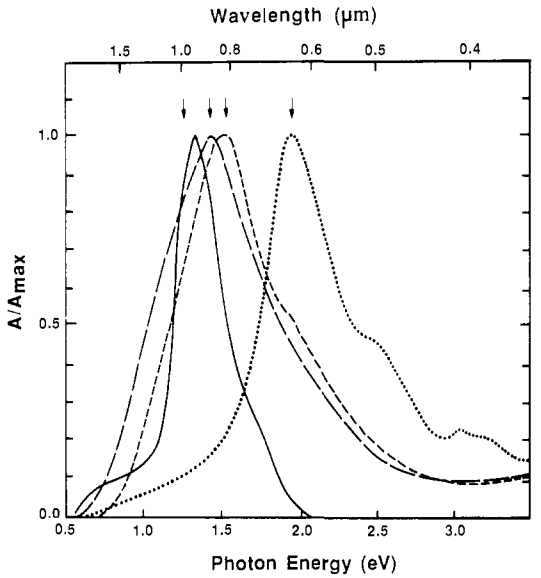

Figure 2. Absorption spectra of thin films which contain $M^+(C222)M^-$. From left to right (peak positions) M = Cs, Rb, K, Na, respectively. The arrows indicate the position of the absorption maxima for the corresponding anions in ethylenediamine solutions. (Adapted from ref 8.)

out with methylamine as solvent at -40 °C for a period of about 24 h. The crystals were obtained by precipitation from a mixture of methylamine and trimethylamine at temperatures of about -70 °C. After removal of the solvent, the product was washed with trimethylamine to remove any excess C222 that might be present. The crystals were manipulated under inert gas and at temperatures below -20 °C to prevent decomposition. They are gold-colored, metallic-appearing crystals which become noticeably yellower and brighter at liquid nitrogen temperatures.

Photoluminescence lifetimes and spectra were measured with a pulsed picosecond laser system. It consisted of a Nd:YAG laser mode-locked at 76 MHz with an average power of 9.4 W (Quantronix Model 416). The pulse duration measured at half-width with a fast diode (Antel AR-S2) and a sampling oscilloscope (Tektronix 7904A) was of the order of 100 ps. The output was frequency doubled and filtered to provide 1.2 W of 532-nm light that was used to pump a dye laser.

A cavity-dumped ultrafast dye laser (Coherent Model 702-2CD) was used to obtain the picosecond pulses. Using rhodamine 6G dissolved in ethylene glycol, wavelengths between 560 and 618 nm could be selected. Pulses with a duration of 6 ps were measured with an optical autocorrelator (Femtochrome FR-103). A cavity dumper was used to extract the laser pulse from the cavity and to reduce the pulse rate. An average power of 50 mW was obtained at a repetition rate of 3.8 MHz. The energy per pulse was of the order of 20 nJ with a corresponding peak power of 7 kW. Most experiments were run at a repetition rate of 1 MHz with an average power of 3 mW, using neutral density filters to attenuate the beam.

The time-correlated single-photon-counting technique was used for the determination of the fluorescence lifetimes.[14] The light emitted by the sample was focused onto the entrance slit of a double monochromator

(14) O'Connor, D. V.; Phillips, D. *Time-Correlated Single Photon Counting*; Academic Press: London, 1984.

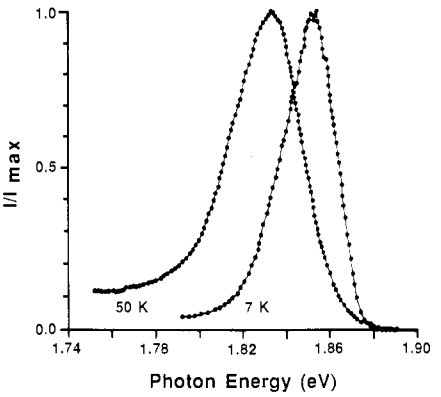

Figure 3. Photoluminescence spectra of $Na^+(C222)Na^-$ at 7 and 50 K, normalized to maximum intensity. The widths (fwhm) are 30 meV at 7 K and 39 meV at 50 K. This increases to 60 meV at 80 K.

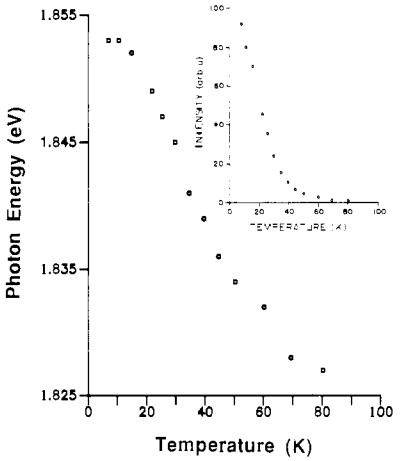

Figure 4. Variation of the photoluminescence peak position for Na^+-(C222)Na^- with temperature. The inset shows the marked dependence of the intensity on temperature.

(Jarell-Ash Model 25-100 equipped with two 1800 lines/mm gratings) to remove scattered light and to provide spectral resolution of 1 meV (0.3 nm). A thermoelectrically cooled photomultiplier (Hamamatsu R955) was used to detect the luminescence signal. A time-to-amplitude converter (PRA Model 1701) and a multichannel analyzer (Nucleus PCA) were used to record the fluorescence decay curves. The conversion gain of the multichannel analyzer was 512 channels, and the time interval per channel was 60 ps. Because of the low emission rates from the sample, the "inverted" configuration of the time-to-amplitude converter was used: the "start" pulse was provided by the photomultiplier and the "stop" signal by the reference photodiode. The signal obtained was displayed in real time on an IBM PC-XT. A rate meter was used to record the steady-state fluorescence spectrum and to monitor the fluorescence efficiency. At 7-9 K the emission rates from the sample were normally in the 1-10-kHz range when the repetition rate of the cavity dumper was 1 MHz.

The instrument response function $P(\lambda,t')$ was measured at the excitation wavelength. The count rate of the photomultiplier was adjusted to that used in actual measurements with appropriate mechanical light stops. The width of the $P(\lambda,t')$ at half-maximum was 400 ps.

Measurements at low temperatures were made in a helium closed-cycle optical cryostat (CTI-Cryogenics). The samples were either attached directly to the coldfinger or were contained in 4-mm quartz EPR tubes filled with He exchange gas. The EPR tubes were clamped onto the coldfinger at -40 °C to prevent decomposition, with a glovebag flushed with pure nitrogen to prevent condensation onto the coldfinger. Initial measurements at 77 K were made with the sample contained in a 4-mm-o.d. quartz tube immersed in a transparent quartz Dewar containing liquid nitrogen. The reported temperature is that of the coldfinger.

Results

A. Steady-State Fluorescence Spectra. At temperatures below 80 K the most intense feature of the emission spectrum is a narrow peak whose position varies with temperature from 669.1 nm (1.854

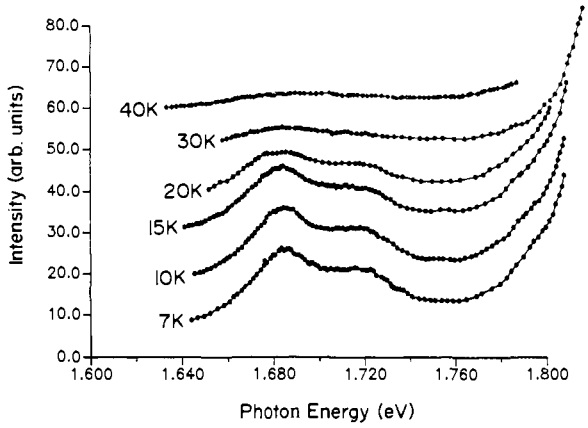

Figure 5. Photoluminescence spectra of $Na^+(C222)Na^-$ between 1.64 and 1.80 eV showing the temperature dependence of the low energy broad peak and shoulder. Note that these features are absent above 30 K. The individual curves are displaced vertically for clarity.

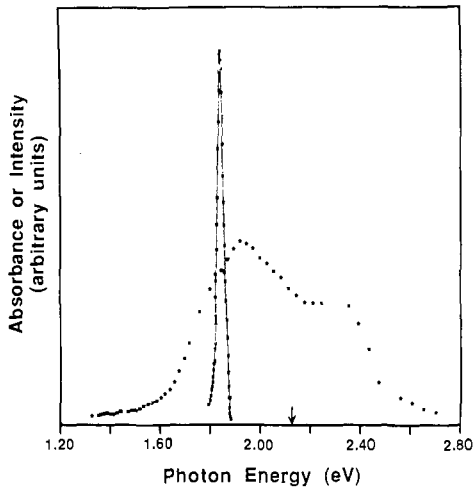

Figure 6. Absorbance (broad curve) measured at 250 K and photoluminescence (sharp curve), measured at 7 K. The excitation energy for photoluminescence is indicated by the arrow.

eV) at 7 K to 678.6 nm (1.828 eV) at 80 K. At the same time, the intensity decreases markedly and the width (fwhm) changes from 30 to 60 meV (about 10 to 20 nm). The spectra at 7 and 50 K are shown in Figure 3. The variation of the peak position with temperature (Figure 4) is approximately linear throughout the whole temperature range. The spectra are asymmetric at all temperatures, with a relatively sharp cutoff toward the high energy side. In addition, as shown in Figure 5, there is a broad peak and a broad shoulder, of much lower intensities, at 1.685 and 1.720 eV respectively. These emissions become negligible above 30 K. In Figure 6, the main emission peak, measured at 7 K, is displayed along with the absorbance, which was measured at 250 K.

B. Photoluminescence Lifetime Measurement. The observed decay curve $I(\lambda,t)$ is related to the real one $G(\lambda,t)$ by the convolution integral:

$$I(\lambda,t) = \int_0^t P(\lambda,t')\, G(\lambda,t-t')\, dt' \qquad (1)$$

The shape of the real decay curve can be obtained by using a nonlinear procedure to fit a trial function $G'(\lambda,t)$ to the experimental data. The experimental results were analyzed by a commercial software program[15] that used the Marquadt algorithm[16] and was capable of fitting up to four exponentials.

(15) James, D. R.; Ware, W. R. *Chem. Phys. Lett.* **1985**, *120*, 455–459. James, D. R.; Demmer, D. R. M.; Verrall, R. E.; Steer, R. P. *Rev. Sci. Instrum.* **1983**, *54*, 1121–1130 (PTI Lasers, London, Ontario).

(16) Bevington, P. R. *Data Reduction and Error Analysis for the Physical Sciences*; McGraw-Hill: New York, 1969.

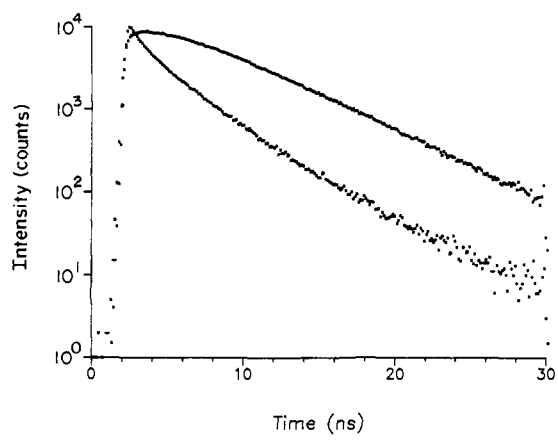

Figure 7. Decay curves (semilog scale) measured at 668.8 (lower) and 675.4 nm (upper). The curve at 668.8 nm has biphasic decay, while the curve at 675.4 nm shows growth followed by decay.

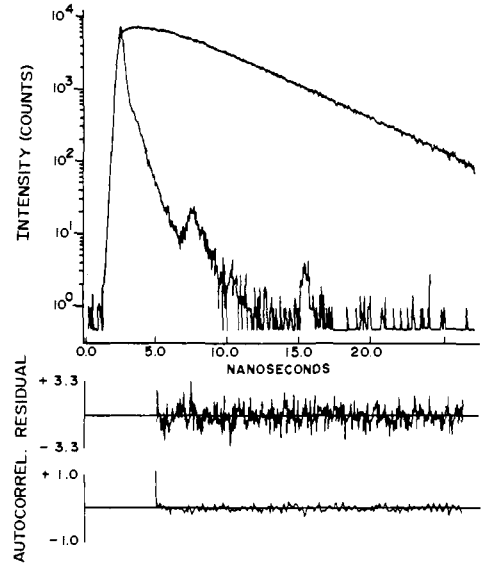

Figure 8. Luminescence decay curve for $Na^+(C222)Na^-$ at 675.4 nm and instrument response function (semilog scale). The deconvoluted fit of this decay to eq 2 gave $\alpha = -1.38$ (3), $\tau_\alpha = 2.36$ (7), $\beta = 2.38$ (5), $\tau_\beta = 4.83$ (2), $\chi^2 = 0.987$. (The numbers in parentheses are the estimated standard deviations of the last significant figure.) Plots of the weighted residuals (RESIDUAL) and the autocorrelation function (AUTOCORREL) are also shown.

Photoluminescence decay curves were recorded at 0.65-nm intervals between 659.0 and 691.8 nm at 7 K. Typical decay curves, measured at 675.4 and 668.8 nm, are presented in Figure 7. Note the change in shape and the shift of the time of maximum signal with wavelength. A representative fitting result is displayed in Figure 8, which also shows the time region over which the data were analyzed. At every wavelength, over the time range used, the experimental decay can be well represented by using for $G(\lambda,t)$ an equation of the form

$$G(\lambda,t) = \alpha(\lambda)\exp(-t/\tau_\alpha) + \beta(\lambda)\exp(-t/\tau_\beta) \qquad (2)$$

Figure 9 shows the variations of the four parameters α, β, τ_α, and τ_β with photon energy, along with the integrated emission spectrum. Note that τ_α and τ_β are nearly constant except on the high energy edge of the spectrum, where both decrease. While the preexponential corresponding to the long-lived component remains positive over the entire range, that of the short-lived component changes sign. This corresponds to an intensity *increase* with time at low energies and a decrease at high energies. Of course, at the crossing point the decay becomes a single exponential.

C. Time-Resolved Fluorescence Spectra. The PL spectrum vs delay times was determined for delay times between 0 and 28 ns. For each delay time, integration was performed over a window

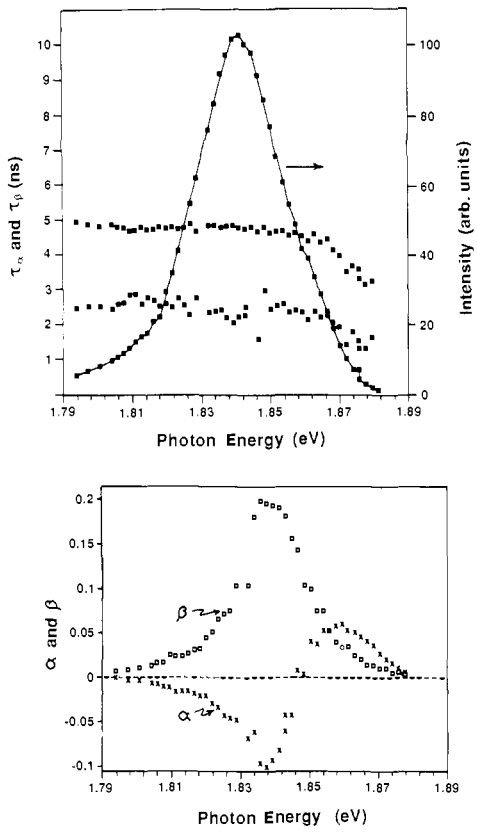

Figure 9. Top: Integrated emission spectrum and parameters of the two-exponential fit to the decay as functions of the photon energy. Values of τ_α (short) and τ_β (long) are superimposed on the spectrum. Bottom: The preexponential parameters $\alpha(\lambda)$ and $\beta(\lambda)$ obtained from the least-squares fit. Note that $\alpha(\lambda)$ changes sign corresponding to growth at low energies and decay at high energies.

of 240 ps. As shown in Figure 10, the PL peak shifts to lower energies as the delay time increases, and the energy shift becomes almost complete after a delay of approximately 10 ns. The total energy shift is about 20 meV (15 nm).

Discussion

The experiments reported here used light of lower energy than the apparent bandgap, as determined by the temperature dependence of the conductivity.[11] The excitation energy was, however, higher than the energy of the absorption maximum, situated at 1.9 eV (650 nm; see Figure 6). Independent measurements with a continuous-wave krypton laser at 647.1 nm (1.916 eV) gave the same photoluminescence spectrum as reported here.[17] Time-resolved emission spectra as well as the variation of the decay profiles with wavelength clearly indicate that this band is complex with at least two emission energies. The breadth of each underlying component is too great compared with the peak separation to permit direct resolution. Variation of the spectrum with time does, however, permit separation of the overall emission spectrum into its components.

Since the spectrum does not change after 10 ns, the shape at long times is that of the long-lived component. The spectrum of the short-lived component can be obtained by subtracting the contribution of the long-lived component from the short-time experimental spectrum. The factor by which the spectrum of the long-lived component was scaled was chosen to bring the base line at low energies to 0. The two components of the emission spectrum are shown in Figure 11. It should be noted that the *short-time* spectrum obtained in this way is somewhat dependent on the experimental spectrum used to obtain it. In particular, the high energy edge becomes more pronounced at short times, indicating the presence of additional short-time emission processes.

The analysis of the decay as a function of the PL wavelength provides additional evidence for the existence of at least two deexcitation processes. At 7 K, the decay curves obtained on the

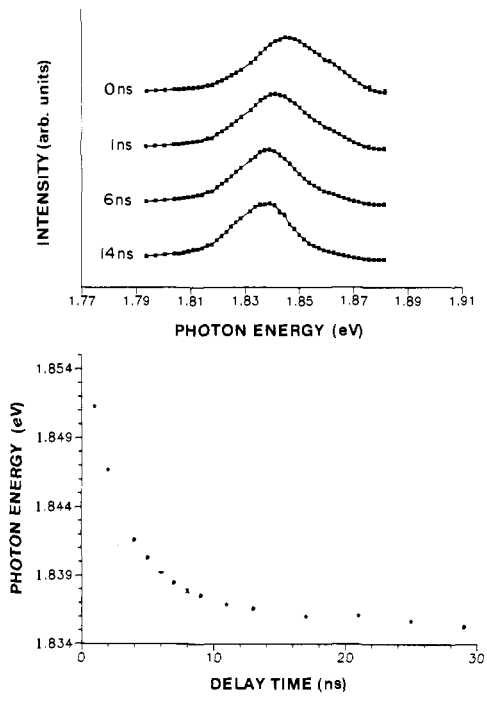

Figure 10. Shift of the emission peaks with time. The top figure shows the spectrum at various times after the excitation pulse as reconstructed from the decay curves. The bottom figure shows the variation of the peak position with time. In the top figure the individual spectra have been shifted vertically for clarity.

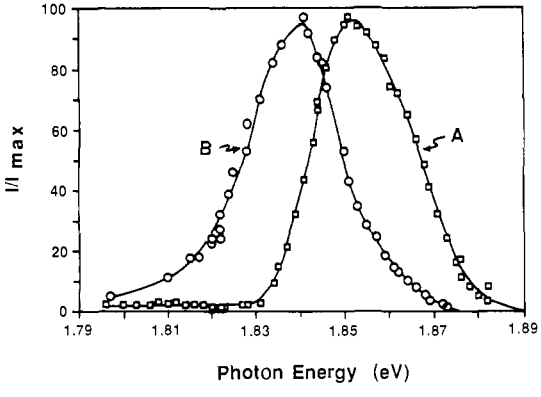

Figure 11. Normalized peak shapes for the short-time (A) and long-time (B) components of emission. The asymmetry on the high energy side of the spectrum and the nonconstancy of the shape of the short-time component suggest that this emission is not from a single state.

high energy side of the peak can be described by two parallel first-order processes with positive values for both preexponentials α and β. On the low energy side, however, the short-lived contribution becomes negative, indicating the growing-in of luminescence at longer wavelengths. These observations are consistent with the mechanism illustrated in Figure 12.

State A is populated after the absorption of a photon of light. The system can then return to the ground state with a rate constant k_1 by emission of light. Alternatively, it can be transformed via a radiating or nonradiating process to another state B, and this transfer is characterized by a rate constant k_2. Subsequently, state B returns to the ground state with emission of light through a first-order decay having a rate constant k_3.

With such a two-state model, the luminescence intensity at any wavelength and time is given by

$$I(\lambda,t) = a(\lambda)\, N_A(t) + b(\lambda)\, N_B(t) \qquad (3)$$

where $a(\lambda)$ and $b(\lambda)$ are characteristic shape functions of the

(17) DeBacker, M. G.; Romain, F., unpublished results.

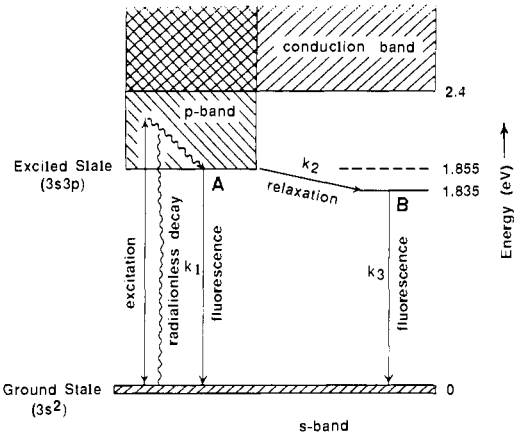

Figure 12. Schematic representation of the decay scheme proposed for the luminescence of $Na^+(C222)Na^-$.

luminescence spectra of the two states. The concentrations of the emitting states $N_A(t)$ and $N_B(t)$ can be derived for the proposed mechanism from the following expressions:

$$N_A(t) = N_A(0) \exp[-(k_1 + k_2)t] \quad (4)$$

$$d(N_B)/dt = k_2 N_A - k_3 N_B \quad (5)$$

which can be solved to give

$$I(\lambda,t) = N_A(0)[a(\lambda) - b(\lambda)k'] \exp[-(k_1 + k_2)t] + [N_B(0) + k'N_A(0)]b(\lambda) \exp(-k_3 t) \quad (6)$$

Equation 6 has the form of the experimental decay curve, eq 2, with the lifetimes being given by

$$\tau_\alpha = 1/(k_1 + k_2), \quad \tau_\beta = 1/k_3, \quad k' = k_1/(k_1 + k_2 - k_3)$$

It is evident from the values of τ_α and τ_β obtained from the decay analysis (Figure 9, top) that k' is a positive number independent of the wavelength and that the sign of the preexponential term is governed by the sign of $a(\lambda) - b(\lambda)k'$ Our measurements do not allow separation of the constants k_1 and k_2.

As can be seen from Figure 9, the extreme high energy side of the emission peak yields lower values of τ_α and τ_β than are obtained over most of the energy range. This decrease is reproducible, cannot be described by a single exponential, and probably represents emission from other states. Attempts to use three or four exponentials were unsuccessful. As indicated above, these processes could also be responsible for the time dependence of the spectral shape of the short-lived component.

The luminescence processes are presumed to occur by first populating excited states in the p band by the absorption of photons ($s^2 \rightarrow sp$). Short-time emission may occur from these states, but the bulk of the emission (rate constant k_1) is from the bottom of the p band (state A) to the relatively narrow s^2 ground state. State B, at slightly lower energies, evolves from state A as the surroundings relax with rate constant k_2 in the presence of the new charge configuration created by the photoexcitation. The rate constant for luminescence from the relaxed state B is k_3.

That the model described above is not a complete description of the luminescence processes is indicated by the time-dependent spectral shape of the short time component (peak A in Figure 11) and the decrease in τ_α and τ_β above $E = 1.87$ eV (Figure 9). The luminescence intensity in the high energy "tail" is very low, however (Figures 3 and 9), and it is difficult to separate the observed emission into more than two components. The extra emission could be from precursor states in the p band. Alternatively, it could arise from the low energy "tail" of a higher energy broad emission that results from photochemical modification of the surface as described below. In any event, it is only a small contribution to the overall emission processes.

The dramatic decrease in fluorescence intensity with temperature emphasizes the importance of nonradiative decay processes. Preliminary experiments show that the long-lived decay time is relatively independent of temperature so that the important nonradiative decay processes must occur from precursor states.

The broad featureless luminescence of $Na^+(C222)Na^-$ previously reported[13] was also observed in these studies, but only for samples that had been at room temperature for some time or when the sample had been exposed to laser intensities of 100 mW or more. In the latter case, photochemical modification of the surface occurred, with a color change from gold to black. The wavelength of a resulting broad emission peak depended upon the excitation energy, ranging from 1.98 eV for excitation at 2.175 eV to 2.35 eV for excitation at 2.542 eV. The origin of this luminescence from photochemically modified crystals is unknown. The effects of laser energy and intensity as well as time-resolved studies at other temperatures are currently under investigation.

Acknowledgment. This research was supported in part by the U.S. National Science Foundation Solid-State Chemistry Grant No. 87-17763 and by the Michigan State University Center for Fundamental Materials Research.